Chapter 1 : CMS and the LHC

1.1. The LHC

Starting in 2007 and for the next few years, the High Energy Physics community will look towards events and reactions at CERN's Large Hadron Collider.

Indeed, the LHC will collide protons together at an unprecedented center-of-mass energy of 14 TeV. The bunch spacing will be of 25 ns, leading to a luminosity of 2 10^{33} $cm^{-1}.s^{-1}$ in the beginning and raised afterwards to 10^{34} $cm^{-1}.s^{-1}$ (100 pb^{-1} per year). The centre of mass energy, combined with the high luminosity will give a unique opportunity to investigate and study new Physics, even very rare events.

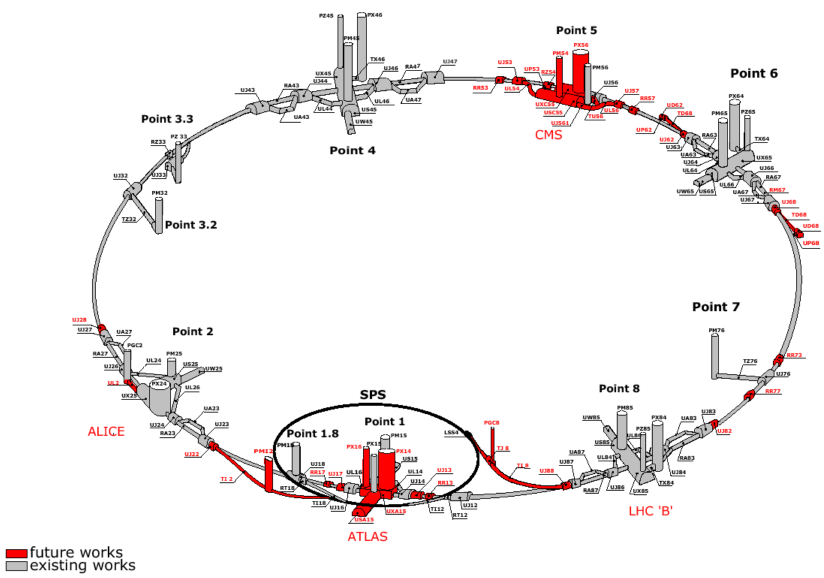

Fig. 1 : The LHC underground installations. The grey structures were already existing at LEP.

The LHC (Fig. 1) will be located in the 27 km-long circular tunnel previously drilled for LEP, but additional caverns and surface structures have been excavated to meet the larger space requirements of the new experiments and to house the necessary services needed to cool down an all-superconducting accelerator.

During operation at high luminosity, there will be no less than ~20 min bias events per bunch crossing, ~1000 charged tracks per event in each experiment. This qualifies the LHC as the most severe radiation environment that any High Energy Physics experiment will have to undergo so far. This latter point is discussed in 1.2.2. while this section focus mainly on the Physics motivations to build the LHC.

For sure the hottest topic at LHC will be the search of the last missing piece of the standard model: the Higgs boson. Its mass is not predicted by theory although there are already constraints coming from previous experiments: we know from LEP that the mass of the Higgs boson should be above 114 GeV. The ignorance of the Higgs boson mass leads to the fact that various scenarios have to be considered and the study of many discovery channels is required, as presented in Fig. 2.

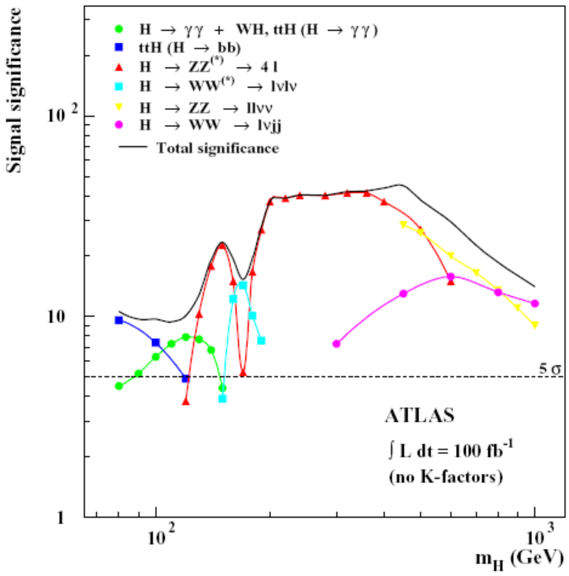

Fig. 2 : Signal significance of the various SM-Higgs discovery channels, after one year or 100 fb^{-1} (from [7]).

The different channels pictured in Fig. 2 can be dispatched into different categories according to the Higgs production mechanism. For instance, a Standard Model (SM) Higgs can be produced through the fusion of two gluons (gluon fusion channels), or via quark interactions in the weak boson fusion channels:

The three gluon fusion channels are:

$gg \rightarrow H \rightarrow \gamma\gamma$ (for $m_H \leq 150$ GeV)

$gg \rightarrow H \rightarrow ZZ^* \rightarrow 4l$ (for $m_H \geq 120$ GeV)

$gg \rightarrow H \rightarrow WW^* \rightarrow l\nu l\nu$ (for $m_H \geq 130$ GeV)

The weak boson fusion channels are:

$qq \rightarrow qqH$, then $H \rightarrow \gamma\gamma$ (for $m_H \leq 150$ GeV)

$qq \rightarrow qqH$, then $H \rightarrow \tau\tau$ (for $m_H \leq 150$ GeV)

$qq \rightarrow qqH$, then $H \rightarrow e^{\pm}\mu^{\pm}\ p_{t,miss}$ (for $m_H \geq 110$ GeV)

$p_{t,miss}$ is missing transverse momentum.

There are even more channels, involving for instance the Higgs decay into a pair of b quarks after a WH or a ttH production:

$q\bar{q} \rightarrow WH$, then $H \rightarrow b\bar{b}$ (for $m_H \leq 120$ GeV)

$q\bar{q} \rightarrow t\bar{t}H$, then $H \rightarrow b\bar{b}$ (for $m_H \leq 130$ GeV)

show that a high resolution tracker is a key subdetector.

These channels, part of the Standard model studies at LHC, already show that LHC detectors must be built according to the present state-of-the-art technology. Every sub-detector plays a crucial role as the exciting perspectives requires the observation of many different decay channels involving photon, quark (jet) and lepton measurements in turn, hence requiring good calorimeters, accurate trackers and an efficient muon system. Many of the decay channels also involve the measurement of missing energy or transverse momentum, hence requiring a detector as “particle-tight” as possible.

The purpose of this section is not to survey the entire Physics program. It is however worth to mention that, besides the SM Higgs discovery, there are numerous extensions to the standard model, among which supersymmetry. This extension assumes that each fermion has a boson counterpart (the squarks and sleptons), and the standard model bosons have fermionic superpartners (gluinos and gauginos). This theory, to be confirmed, implies the discovery, the identification and study of a whole new spectrum of particles, including no less than 5 Higgs particles. The entire parameter space of the minimal supersymmetric model (MSSM) can be studied at LHC and hence if supersymmetric higgses exist, some of these have also to be observed at LHC [8].

Apart from supersymmetry, numerous exotic models are proposed as extensions of the standard model (refer e.g. to [7], [8] or [9]). A possibility would be to consider a fourth generation of leptons and quarks. Predictions on a fourth generation of quarks show a dominant decay mode to Wb. Hence again, the detection of secondary vertices and an accurate tracking are needed.

Other model predicts the existence of new heavy gauge bosons (W' and Z', with a mass of several TeV) or even magnetic monopoles, leptoquarks (particles carring both a leptonic and a baryonic quantum number)… There is also the so-called Technicolor, a new strong interaction at high energy scales that gives a possible alternative to the Higgs mechanism of electroweak symmetry breaking but implies the existence of specific technifermions.

Furthermore, if the presence of extra-dimensions is observed in collider experiments, it may be a major step towards a unified theory of the fundamental interactions. Hence they will be studied at the LHC, both in direct (cf. [10]) observation channels and indirect ones (cf. [11]).

As far as the tracker is concerned, the need for resolution is clearly seen in channels involving lepton identification – for instance, the accurate identification and reconstruction of electrons implies a good separation with photon events in the electromagnetic calorimeter- but even more in the channels involving the secondary vertex measurements, as is the case for detecting the b quarks. The tracker is also used for jet isolation, and even at low Higgs mass, for $H\to\gamma\gamma$ it is useful to calibrate the electromagnetic calorimeter. The CMS collaboration decided the following design guidelines (cf. [13]):

- The leptons should be measured up to η=2.5, hence the tracker has to cover the pseudorapidity range up to at least this value.

- The transverse momentum P_t resolution should be better than 1 % below 100 GeV for an intermediate mass Higgs discovery.

- A z-resolution of 2 cm for the primary vertex is a minimum requirement. This implies a tracker with small cells coupled to an efficient and robust pattern recognition algorithm due to the pile-up.

- A fast response time is needed due to the high data acquisition frequency.

- The material budget must not be neglected and kept as low as possible as this is a crucial factor in the energy resolution for electrons and gamma measurements.

1.2. Zoom on CMS

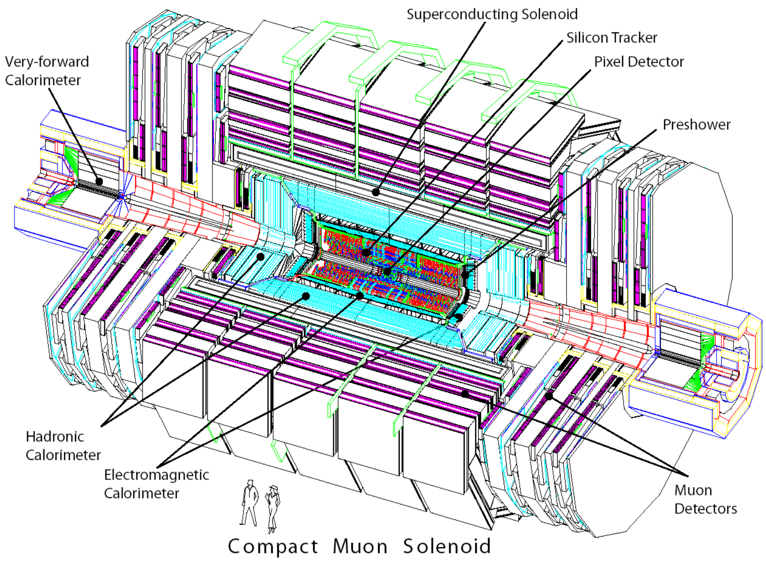

Fig. 3 : Layout of the CMS experiment at LHC.

The Compact Muon Solenoid will be one of the four LHC experiments. It is a multi-purpose particle physics detector based, like any modern High-energy Physics experiment, on an onion-like structure. One of its peculiarities is its innovative design, based on new technologies used at a large scale. A sketch of the experiment is shown on Fig. 3. This paragraph is aimed to describe briefly the different sub detectors making CMS.

Starting from the outer part and successively "removing" in turn all the layers of our "onion", the first and most external sub detector encountered is the muon system. Indeed, muons are, right after the undetected neutrinos, the most penetrating particles produced at LHC. The outermost detectors, placed in the gaps of the return yoke, are hence dedicated to the tagging of these muons. In the case of CMS, the muon system consists of drift tubes (DT) in the barrel (up to η=1.2) and cathode strip chambers (CSC) in the endcaps, up to η=2.1. Additional resistive plate chambers (RPC) are used for bunch identification.

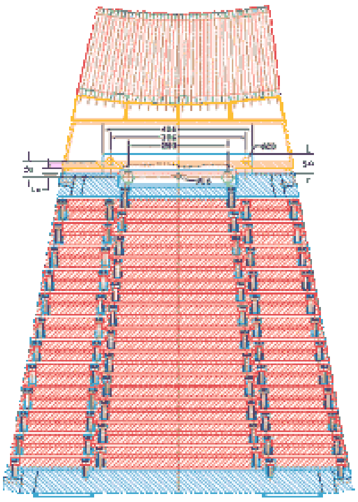

Fig. 4 : A slice view of the HCAL Barrel: copper plates interleaved with plastic scintillators sheets. Copper plates are 50 mm thick whereas scintillator plates are 4 mm thick. The readout uses plastic wavelength shifting fibers.

Right inside the muon system, one finds the outer barrel of the hadronic calorimeter, installed there because HCAL is only about 6.5 radiation lengths thick. Removing this outer barrel uncovers the superconducting magnet. It will be one of the biggest and most powerful magnet ever built, able to deliver a magnetic field of 4 Tesla in a volume about 355 m^3. This magnet contains the calorimeters for energy measurements. It implies that the sensitive elements of the calorimeters will operate in a high magnetic field, hence narrowing the choice of technology for the detectors to be used.

With the magnet yoke "peeled off", we now look at the hadronic calorimeter. It is a sampling calorimeter made of successive layers of copper plates (radiator) and plastic scintillator sheets with a wavelength-shifting fibre readout. HCAL covers all directions up to $\eta=3$. At high η, in the very forward calorimeter, copper is replaced with steel to minimize activation problems and the scintillators are replaced by quartz fibers, able to sustain higher radiation doses. Due to the high magnetic field, the fibres are readout using hybrid photodiodes ("HPD"[¤]). The granularity of the calorimeter, corresponding to an array of 5X5 cm^2 crystals, is about 0.087 by 0.087 in η and Φ[*].

Going deeper inside, the next item found is the electromagnetic calorimeter. It has been optimized for the $H\rightarrow\gamma\gamma$ decay channel since a mass resolution of $\Delta m_H/m_H < 1\%$ has to be achieved [8]. This calorimeter is made of more than 80000 $PbWO_4$ crystals. Despite their low light emission level, they are a good choice because of their small radiation length (allowing a compact calorimeter design[*]), their small Molière radius (22 mm), their fast response and the good light collection (most of the light yield is collected within the 25ns bunch spacing).

CMS is monitored by different control systems to ensure a high accuracy of the measurements. For example, in the case of ECAL, the optical transmission of the crystals drifts with time and is therefore continuously monitored by means of light pulses that are injected using clear optical fibres. This interesting feature is pictured on Fig. 5. In the case of the tracker, the alignment and positioning of the different structures relative to each other and to the rest of the detector is continuously monitored by multiple infrared laser beams [14] that are seen by dedicated silicon sensors called "optical sensors".

[¤] HPD's are made of a photocathode and a diode separated by a gap of a few millimetres. A high electric field is applied between cathode and diode, so that photoelectrons are accelerated before being detected by the diode. In contrary to photomultipliers, a high axial magnetic field can be tolerated by these devices.

[*] It is usual to use cylindrical coordinates. In that case, z is the longitudinal distance in the beam direction, r is the radial distance and Φ the corresponding angle.

[*] The measurement of the energy in Ecal requires the crystals to be as long as 26 radiation lengths. In the Case of $PbWO_4$, this gives only 23 cm long crystals.

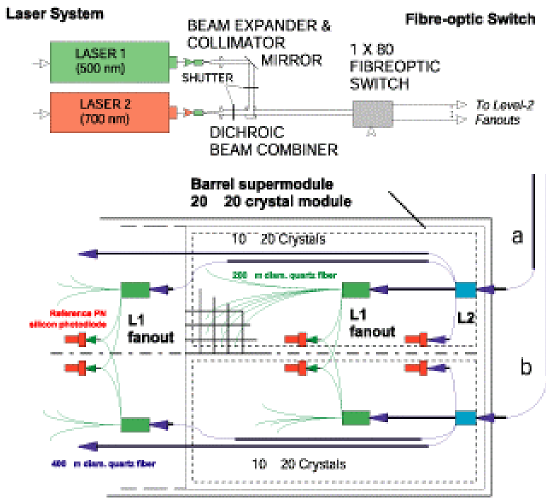

Fig. 5 : Light monitoring system of the CMS electromagnetic calorimeter. LASERs are used as light source and distributed over the entire calorimeter using optical switches and fanouts.

In addition to the ECAL crystals, there is a preshower detector in the endcaps to allow the separation of photon pairs, neutral pions and single photon events. This preshower detector consists of two layers of silicon strip detectors with orthogonal orientations, sandwiched between two lead sheets.

The inner tracking system is located further inside the calorimeters. It consists of the tracker and the pixel detectors. As the silicon strip tracker will be further described in paragraph 1.2.1, we will only say a few words about the pixels here.

The pixel detector (Fig. 6) is located as close as possible to the interaction point. It will be 120 cm-long, with an inner diameter of 8cm. The main purpose of this detector is the accurate determination of the vertex positions that are crucial for e.g. *b*-jet tagging (crucial for instance in the study of $H \rightarrow b\bar{b}$). To fulfil its role, it is designed to deliver 2 hits per track up to a pseudorapidity of η=2.2. With a pixel size of 150X150 µm², the high accuracy of the hit position is reached thanks to a signal interpolation between pixels, improved by the Lorentz-angle effect. This is the reason for choosing a turbine-like geometry for the disks. The induced charge division between adjacent strips, coupled with their analogue readout, enhances the accuracy in the particle crossing position to as low as about 15 µm, giving a resolution of about 50 µm for the transverse position of the vertex.

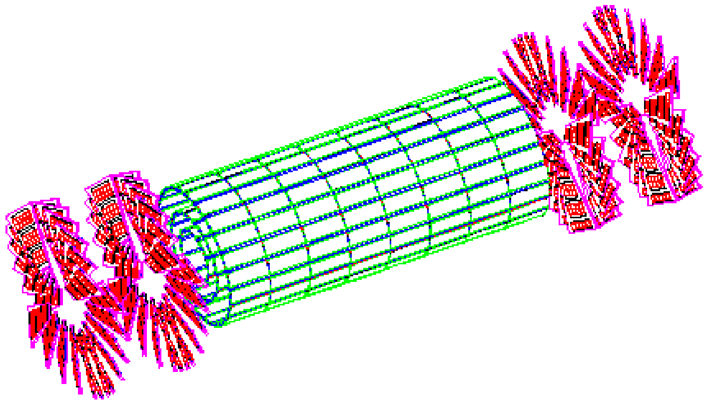

Fig. 6 : The CMS pixel detector layout. One distinguishes the three barrel layers and the two turbine-like endcaps on each side.

1.2.1. The CMS tracker

In 2000, the CMS collaboration decided to build an all-silicon tracker, putting aside the MSGC detectors. In the new design, the CMS tracker is subdivided in several different parts, namely (from the interaction point towards the calorimeter): the inner barrel, closed by 3 small disks on each side; the outer barrel; and the endcaps. This tracker will be the biggest all-silicon tracker ever built with about 11.4 10^6 channels and an active surface of more than 200 m².

The inner part of the tracker consists of a barrel (TIB) with four layers of silicon modules arranged in concentric cylinders, flanked by three disks (TID) of three concentric rings of modules on each side. The sensors used to build the inner tracker modules are all 320 µm thick with low resistivity silicon wafers.

The outer part of the tracker is also made of a barrel (TOB) consisting of six concentric cylinders whereas the endcaps (TEC) are made of nine disks on each side, with seven rings of modules per disk. All modules will be built with 500 µm thick, high resistivity sensors apart the four innermost rings of the endcaps that will be assembled with 320 µm thick sensors because they are closer to the interaction point.

Fig. 7 shows the sketch of a quarter of the tracker together with the pixel detector. Starting from the interaction point in the lower left corner, one distinguishes the pixel detector, and thereafter the inner barrel, closed by the inner disks, and the outer barrel, closed by the endcaps.

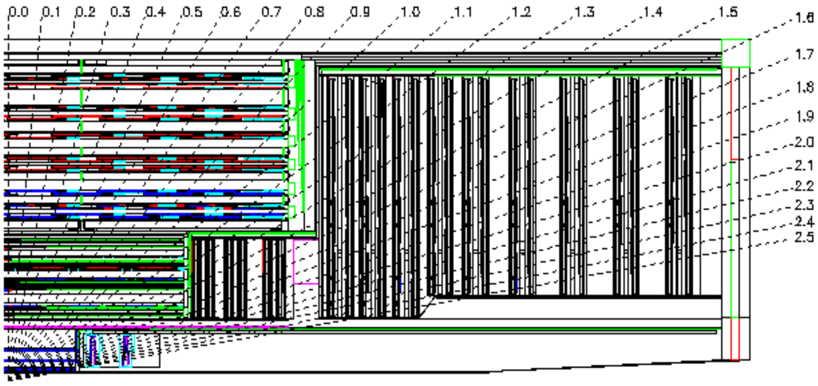

Fig. 7 : Transverse view of the CMS tracker. The radius is about 115 cm and the length about 270 cm on each side of the IP.

Looking further into the details of the tracker construction, we will first describe the support structures, going into more details on the detector modules thereafter.

The support structure of the tracker has to carry all the detectors, data and controls cables but must also respond to additional requirements:

- It houses the pipes of the cooling system to keep the tracker at a temperature of -10 °C in its entire volume of 24.4 m^3. Cooling will be needed to avoid reverse annealing of the depletion voltage of the silicon sensors (cf. 2.3.3.b) and also limit the leakage current (cf. 2.2.2), hence ensuring the detector to be kept fully depleted and limiting the noise in the mean time. The cooling power must be large enough to cope with the increased power consumption over the years* of operation and avoid thermal runaway.

- The temperature requirement implies that the tracker must be operated in a controlled dry atmosphere to avoid condensation on the sensors and electronics.

- The support structure has to be stiff enough to guarantee the accuracy of the position measurement of the tracker. One of the stringent requirements for this is the minimal deformation with

* The foreseen total power consumption of a petal after 10 years of use is about 70W for a "back" petal, 90 W for a front petal.

temperature cycling and a high stability versus time. The positioning precision of a module must be about 100 µm with time variations in the 10 µm range [17].

- The high magnetic field requires also the use of paramagnetic materials to limit stresses on the structure.

All these features have to be achieved with a mass as low as possible to limit its contribution to the material budget.

In the case of the CMS support structure, both the inner and outer barrels are made of a skeleton that supports the carbon fiber “rods” onto which the modules are attached. Inner and endcap disks are made of honeycomb panels with carbon fiber skins to ensure the stiffness. In the case of the TEC disks, the modules are arranged in “petals” fixed to the disks. These support structures are shown on Fig. 8.

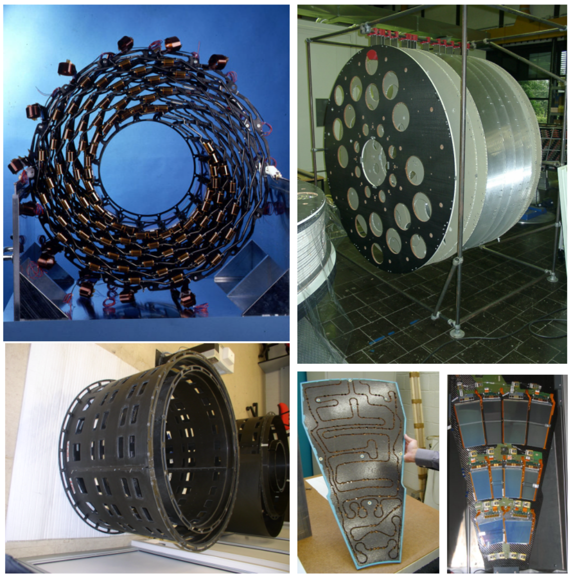

Fig. 8 Clockwise from bottom left: support structure of TIB, support structure of the TOB filled with some rods, TEC honeycomb support disk, TEC petal with modules, details of the cooling pipes grooves of a TEC petal.

As shown on the picture above, the low temperature operation of the tracker is obtained by the circulation of a cooling fluid. Despite the difficulties encountered at welding and soldering the pipes to their connectors, titanium has been chosen as a material for the endcap pipes due to its good radiation resistance, its absence of induced long-term radioactivity, its low mass and easy bending properties.

A module is the most basic yet fully functional detection unit of the tracker. It is made of a high thermal conductivity carbon fiber frame which supports one or two silicon sensors connected to their readout electronics using a pitch adapter.

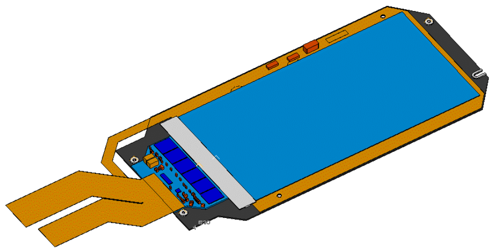

Fig. 9 : Drawing of a CMS barrel module. One can distinguish the carbon-fibre frame with the silicon sensors and their readout electronics.

There are several modules geometries within the tracker: 4 rectangular types are used to build the barrel, and 7 wedge-shaped are mounted on the petals of the endcaps. Among the different layers made of these modules, several are equipped with double sided (stereo) modules. A double sided module has twice the number of silicon sensors as a normal module: the microstrip sensors are mounted back to back and their strips are tilted by a relative angle of 0.1 rad to give a 3-D information about the particle crossing. The pitch of the sensors is higher in the outer parts of the tracker, where the need for high resolution is lower.

It is time now to focus on the tracker readout scheme. Sketched on Fig. 10, the readout electronics in the CMS tracker features several modules: the control (FEC-front end controller) and readout (FED-front end driver) systems are located outside the detector and get or send their information using numerous monomode optical fibres coming in and out of the tracker. Inside the detector itself, the control of the modules is made by the CCUs (clock control unit) that, for instance, distribute the clock and trigger signals. The module electronics performs the strip readout and local storage of the analogue data (analogue pipeline voltage-APV chip), but also integrates the controls and the multiplexers used to send the signals to the optical transmitters that gather signals from the modules and are in charge of sending the data to the counting room. After shaping, the signals of all strips are multiplexed and sent to the underground counting room via single mode optical fibres. This transmission mode has been chosen for its minimal contribution to the material budget and its immunity to electrical interferences.

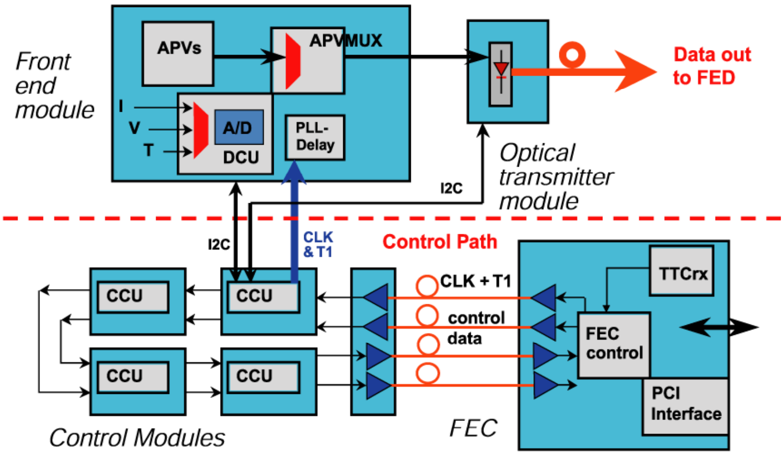

Fig. 10 : CMS tracker electronics overview.

All the different module types have a single readout scheme, using the same APV chip, described for example in [18]. Each strip on the sensors is connected to a charge sensitive amplifier and shaper sampled at 40 MHz and whose output is stored in an analogue pipeline, waiting for he L1 trigger.

Under normal running conditions, the APV shows a very good linearity: better than 5 %. It can be run in 3 different filter modes: peak, deconvolution and multi-mode:

- In peak mode, the signal amplitude of a single bunch crossing is recorded. In the absence of pile up, this gives a better signal to noise ratio and hence a better position resolution than the other modes.

- In deconvolution mode, the signal is shaped using three bunch crossings. The data of the three bunch crossings are stored on 3 capacitors of different values and the chip then outputs a weighted sum of the signal. This gives a better timing accuracy and removes the effects of pile-up but weakens somewhat the position resolution. At high luminosity, the signal to noise performance of tracking is decreased due to pile-up. The deconvolution mode allows to diminish pile up effects, and the S/N ratio is 1.7 times higher in this mode than in the peak mode.

- The multi-mode operation can be used when calibrating the pulse shape. In this mode multiple consecutive pipeline columns (corresponding to multiple bunch crossings) can be read without filtering.

The APV is implemented in 0.25 μm technology, which ensures a good noise performance and a high radiation tolerance by nature and design. By nature because the miniaturization of the chip reduces the oxide layers sizes and thicknesses, hence reducing the amount of charge trapping due to the exposure to radiation: the effects of radiation drop as the square of the oxide thickness and for very thin oxide layers (<10 nm, which is the case of the APV25), most of the charges drift away in a few minutes. Nevertheless, some design rules have to be taken into account to reinforce the radiation hardness, such as p^+ guardrings and enclosed transistors geometries to avoid leakage current paths. Such design rules also prevent the chip to be sensitive to single events effects (SEE*): for instance a test at PSI predicted a worst-case LHC scenario of 84 SEU/hour over all the 2000 CCUs of the tracker.

We already stated the requirements of the tracking system, among which the material budget. With all its features and the electronics described above, Fig. 11 shows the material budget of the CMS tracker for its different components in terms of radiation lengths [16].

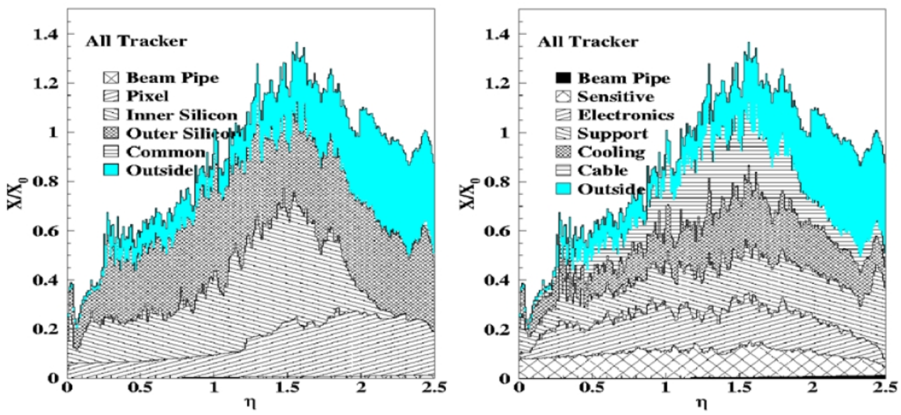

Fig. 11 : the tracker material budget distribution, expressed in terms of radiation lengths [16]. The photon attenuation length due to pair production is approximated by 7/9 the radiation length. At η=1.5, the photon attenuation is hence about 16 %.

* Short definitions of Single Event Effects is given at the end of this document.

As a general rule, the resolution of a tracker is proportional to:

$$\frac{\sigma_{p_t}}{p_t} \propto \frac{\varepsilon p_t}{0.3BL^2} \qquad (1.1)$$

Where p_t is the transverse momentum; σ_{pt} the error on the transverse momentum; ε, the error on the position perpendicularly to the track; B, the magnetic field and L, the track length. In the case of CMS, with a nominal magnetic field of 4 T and a radius of 1.1 m, the resolution of 1 % for tracks with p_t<100 GeV translates into a strip pitch of about 100 µm. (1.1) then becomes [19]:

$$\frac{\sigma_{p_t}}{p_t} \approx 0.12\left(\frac{pitch}{100\mu m}\right)\left(\frac{1.1m}{L}\right)^2\left(\frac{4T}{B}\right)\left(\frac{p_t}{1TeV}\right) \qquad (1.2)$$

As an example of the role of material budget in the performance of the tracker, The p_t resolution given by (1.2), valid in the case of a material-less tracker, is about 1.2 % for 100 GeV muons at low η, whereas a realistic tracker has a resolution of about 1.6 %.

The accuracy of track measurements has been simulated and studied in the case of muons (cf. [16]). It is foreseen to be between 10% at 1 TeV and 0.1 % at 1 GeV and low η. At high η the resolution lies between 30 and 2 %. The azimuthal angle resolution (Φ) is about the same, but is better for high P_t particles (about 0.01 %) compared to low P_t ones (about 0.2 %). The cotan(θ) resolution has been studied as well.: at low pseudorapidity, it is assessed at 0.05 % at high P_t and 0.2 % at low P_t; for higher pseudorapidity it is of the order of resp. 0.3 % and 2 %.

The track reconstruction efficiency for muons lies between 95 and 99 % depending on the muon P_t and η. When considering jets, the track finding efficiency falls to about 85 %.

These performance data are valid only after the alignment of the tracker, which will be performed at first with a laser beam system, and then, in the early operation of the detector, using real tracks of particle crossing the detector [20].

1.2.2. Radiative environment in the CMS Tracker

It has been pointed out at the beginning of this chapter that the high luminosity and the unprecedented beam energy of the LHC will generate the most difficult environment ever encountered by HEP experiments. It was therefore crucial to assess the fluxes inside the detector, and especially in the tracker, where these fluxes are the most intense. The purpose of this section is to outline the properties of the radiation field as described in [15] and updated in [16].

When considering the radiation hardness issues, dedicated simulations are needed since a non-negligible part of the damage comes from low-energy phenomena which are usually neglected when performing Physics studies. As a striking example, the radiation environment of the inner part of the tracker is dominated by direct contributions coming from the interaction point, but already at a radius of 50 cm, the tracker starts to undergo the intense flux of albedo neutrons generated by hadronic interactions with the ECAL crystals located at larger radii. While the radiation originating from the interaction point is irreducible, a polyethylene shielding is foreseen to limit this albedo neutron flux.

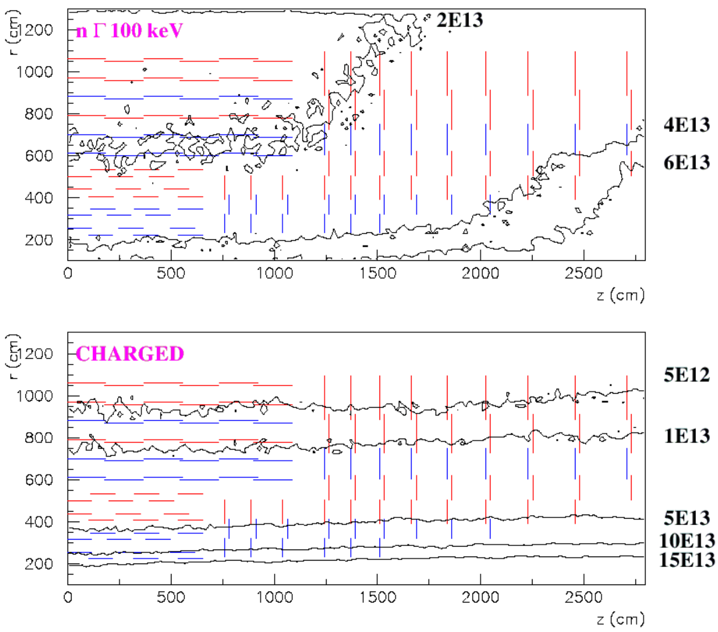

Fig. 12a, b : Neutron and charged particle integrated fluences in the CMS tracker expressed in particles.cm^{-2} after 10 years at the LHC.

Also, the fluxes and fluences obtained during the operation of the accelerator have to take several additional parameters into account: the luminosity variations (high or low luminosity runs and the number of fills per day) and the maintenance periods. All these parameters as well as their uncertainties led to a conservative estimation of the error margins as high as 30 % for the charged particle fluences and a factor 2 may be considered in the case of albedo neutrons.

Starting from these radiation fields, a total dose and fluence are deduced. For given particle types and known energy spectra, one can compute a NIEL normalisation factor (Table 1; more details about the method are given in paragraph 2.3.2).

	$|\eta|$= 0 – 0.9	**$|\eta|$= 0.9 – 1.8**	**$|\eta|$= 1.8 – 2.7**
R= 0 – 20 cm	75	69	62
R= 20 – 40 cm	88	85	82
R= 40 – 65 cm	100	95	92
R= 65 – 120 cm	109	106	104

Table 1 : Average NIEL factors in the tracker (in MeV.mb).

These radiation fields are translated into a 1 MeV-neutron equivalent fluence, which is more convenient regarding the radiation tests (Table 2).

It should already be stressed that the NIEL factors are subject to large uncertainties as the damage functions of all particles over the whole LHC energy range are not well known or experimentally confirmed. Together with the uncertainties on the fluences, a safety factor of 1.5 to 2 should be applied to the 1-MeV equivalent fluence. Hence, as a general rule and for what concerns this thesis, it is usually considered that the inner tracker sensors have to sustain a fluence of 2.4 10^{14} 1-MeVn.cm^{-2} whereas outer tracker sensors one have to sustain 0.5 10^{14} 1-MeVn.cm^{-2} (0.8 10^{14} 1MeV-n.cm^{-2} in the worst outer tracker case). A very conservative approach has hence been considered.

TIB (averaged)					
Radius (cm)	22	32	41	49	58
1-MeV Φ (10^{13} n.cm^{-2})	15.7 ±0.1	8.88 ±0.09	6.22 ±0.05	4.67 ±0.04	3.54 ±0.04

TOB (averaged)					
Radius (cm)	75	85	95	105	115
1-MeV Φ (10^{13} n.cm^{-2})	2.9 ±0.1	2.58 ±0.05	2.36 ±0.05	2.2 ±0.06	2.09 ±0.06

TEC					
Radius (cm)	75	75	75	75	75
Z (cm)	117	141	177	210	255
1-MeV Φ (10^{13} n.cm^{-2})	2.8 ±0.1	3.6 ±0.2	3.7 ±0.4	3.9 ±0.2	4.9 ±0.2

Table 2 : 1-MeV equivalent fluences as quoted in [15] and [16].

The radiation environment also presents another damageable effect on the electronics: highly ionizing particles events (known as “HIPs”). HIP events mainly affect the readout electronics as they can saturate it or cause permanent failures due to large charge depositions (up to 1000 MIPS) in a few channels. In the case of CMS tracker, Monte-Carlo simulations have evaluated the rate of such events, and the effects on the readout electronic were assessed with test-beams at the PSI (see e.g. [23] and [24]). The inefficiency of an APV chip induced by a HIP event is about 20 to 36 % during the 750 ns following the event (the deadtime being raised up to 350 ns). This may be regarded as something catastrophic, but the large number of channels and the presence of several layers of the tracker are such that the actual track reconstruction inefficiencies are at the percent level. The HIP will have therefore a negligible effect on the tracker regarding its Physics performances.